Effects of multipath and antenna on GPS observables

W. Zhuang
J.M. Tranquilla

Indexing terms: Antenna characteristics, GPS observables, Multipath interference

Abstract: The authors present the analysis of multipath and antenna effects on global positioning system (GPS) observables using the functional modelling and simulation package of a digital baseband processor for the GPS receiver. Three issues are addressed: first, the static observable errors as functions of multipath parameters are derived mathematically in the absence of input noise; secondly, the dynamic code and carrier tracking errors as functions of time due to multipath in the presence of input noise are investigated; and finally the deterioration in the accuracy of the GPS observables due to antenna residual phase and antenna centre movement is studied with different receiver design parameters. It is shown that the functional modelling and simulation package provide an alternative approach to GPS system accuracy research where theoretical analysis and hardware methods are very difficult, inaccurate or prohibitively expensive.

1 Introduction

The navigation satellite timing and ranging (NAVSTAR) global positioning system (GPS) is a satellite-based, worldwide, all-weather navigation and timing system. The GPS is designed to provide precise position, velocity and timing information on a global common co-ordinate system to an unlimited number of suitably equipped users [1, 2]. A GPS satellite transmits information to users on two different L-band frequencies, L1 and L2. The dual frequencies permit users to correct for ionospheric delays in signal propagation. The L-band signals are modulated with two pseudorandom noise (PRN) codes: the precision (P) code which provides for precise measurements of the signal propagation time delay and the clear/acquisition (C/A) code which provides for easy code phase lock-on and handover to the P code. The GPS observables include pseudorange between the satellite and the user receiver, the carrier beat phase and Doppler frequency shift of the received signals. A user can obtain his three-dimensional co-ordinates and clock bias correction based on the pseudorange measurements from at least four satellites, and his three-dimensional velocity based on the Doppler shift of the incoming signals. The measurements of the carrier beat phase (between the carrier phases of an incoming satellite signal and the corresponding carrier phase of the user-equipment local carrier oscillator without Doppler shift) enable very accurate measurements of pseudorange variations to be made.

Previous research on the accuracy of the GPS system has presented: first, the effects of signal propagation media from satellites to receiver antennas on the GPS observables; and secondly the accuracy analysis of the GPS observables based on the operation of the GPS receiver hardware, as in references 3–5. In the analysis using a hardware receiver, the receiver is generally assumed to be transparent to the interference at its input. In actual operation, however, because the parameters of the receiver input signal are unknown and the influences of each signal propagation medium on the observables are difficult to detect and remove (due to the stochastic properties of the communication channel and many simultaneous interference sources), the analysis of the GPS observable accuracy includes errors. On the other hand, the theoretical analysis of the system's accuracy has its limitation, due to the difficulties of mathematically modelling some interference sources and the complicated process of each interference source passing through the receiver. For instance, although multipath interference may be characterised by its probability density function, solving mathematical equations for the induced GPS observable errors is not practical (if not impossible): also, it is difficult to mathematically describe some characteristics of GPS antennas, which results in the theoretical analysis of antenna effects being even more difficult or impossible. As a result, computer simulation is an essential approach to studying GPS system performance. By simulating the GPS signals (with interference and noise) passing through the RF, IF and baseband modules of hardware receivers, it is possible to isolate each interference source and to analyse its effects on the GPS observables if the input satellite signal is properly designed. The analysis is accurate because both the input and output signals of the receiver are known, which is impossible to specify with the hardware approach.

The functional modelling of a digital baseband processor (DBP) for the GPS receiver has been developed mathematically and implemented in software [6]. The receiver operates at the L1 and L2 frequencies and using both the P code and the C/A code. The DBP performs the maximum likelihood estimation of the GPS observables. The key components of the DBP are a digital delay lock loop (DDLL) for the pseudorange time delay meas-

Paper 1998F (E15), first received 25th February 1994 and in revised form 23rd January 1995

W. Zhuang is with the Department of Electrical and Computer Engineering, University of Waterloo, Waterloo, Ontario, Canada N2L 3G1

J.M. Tranquilla is with EM Technologies Inc., Fredericton Business Park, 64 Alison Blvd., Fredericton, NB, Canada E3B 5W6

urement and a digital phase-locked loop (DPLL) for the carrier beat phase and Doppler shift measurement. The developed GPS software receiver has been validated by theoretical analysis [6]. In this paper, we apply the receiver function modelling and simulation package to study the effects of multipath interference and GPS antenna characteristics on the accuracy of the GPS observables, which can be further transferred into GPS positioning accuracy.

2 Multipath effects

Multipath is the phenomenon whereby a radio signal arrives at a receiver via two or more of several possible routes with the result that the arriving signals, although having a common time origin at the transmitter, arrive 'out of step' or with a relative phase offset. The multipath phenomenon can cause serious contamination of the receiver observable measurements. Effective approaches to reducing the multipath contamination include designing receiver antenna with a low side lobe radiation pattern and digital signal processing (such as filtering) of the GPS observables [3–5]. Most of the previous research was based on hardware receiver measurement data which is contaminated by GPS signal transmission media other than multipath. Another method of analysing multipath effects is based on multipath modelling and receiver function modelling. The relationship between the multipath patterns and the induced GPS observable errors can be obtained by simulating the multipath signals, which is useful in understanding the multipath effects and in reducing the positioning error due to the multipath. Since multipath modelling is beyond the scope of this paper, the analysis and simulations of multipath effects herein are based on a simplified multipath model. Once other multipath models are developed, the receiver simulation package can be similarly used to perform the analysis.

2.1 Multipath effects in the absence of noise

A simplified multipath model with only one multipath (reflected) signal is chosen, as shown in Fig. 1. In the

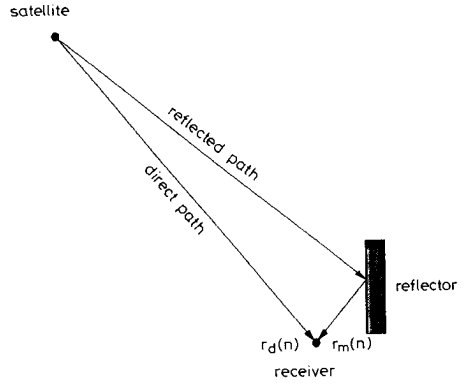

Fig. 1 *Simplified multipath model*

receiver, the DDLL is used to extract the PRN code phase of the input signal which is sampled with a sample interval T_s. The DDLL correlates the input signal samples with the receiver locally generated PRN code signal samples by using an integrate-and-dump filter. The nth sample of the direct input signal component of the DBP in the kth correlation interval is [6]

$$r_d(n) = AP[(1+\zeta)nT_s - \xi T_p] \times \cos[(\omega_b + \omega_{dk})n + \phi(k-1)] \quad (1)$$

where A is the signal amplitude, $P[x]$ is a ± 1-valued PRN code with phase x, $\zeta = f_d/f_L$ (f_d is the Doppler frequency shift and f_L is the RF frequency), ξT_p ($=\tau$) is the code phase delay with respect to the GPS system time (T_p is the code chip width), ω_b ($=2\pi f_b T_s$) and ω_{dk} ($=2\pi f_{dk} T_s$) are the digital radian frequencies corresponding to the baseband carrier frequency f_b and the Doppler shift f_{dk} (of the interval), respectively, and $\phi(k-1)$ is the initial carrier phase of the kth correlation interval (i.e. at $n=0$). The Doppler shift due to the relative movement between the satellite and receiver has a two-fold impact on the received signal: first, carrier frequency offset — the received carrier signal frequency is equal to $f_L + f_d$; and secondly, PRN code chip rate offset — because the PRN code is modulated on the carrier signal, the code rate R of the received signal is equal to $(1+\zeta)R_0$, where $R_0 = 1/T_p$ is the code rate without the Doppler shift. Let α represent the amplitude ratio of the reflected signal to the direct-path signal, $\Delta\tau_m$ the additional time delay of the reflected signal with respect to the direct-path signal, and $\Delta\theta_m$ the carrier phase shift induced by the reflector, and assume that the signal carrier phase delay equals the signal group delay, then the reflected signal input to the DBP is

$$r_m(n) = \alpha AP[(1+\zeta)nT_s - \xi T_p + \Delta\tau_m] \times \cos[(\omega_b + \omega_{dk})n + \phi(k-1) + \beta] \quad (2)$$

where

$$\beta = -(\omega_b + \omega_d)\Delta\tau_m/T_s + \Delta\theta_m \quad (3)$$

is the carrier phase offset due to $\Delta\tau_m$ and $\Delta\theta_m$. The output of the PRN code phase discriminator of the DDLL is [7]

$$D = \frac{A^2}{4}\,\mathrm{sinc}^2[(\Delta\omega_{dk})N/2] \times [R^2(\rho-\delta) - R^2(\rho+\delta)] + D_{err} \quad (4)$$

where $\mathrm{sinc}(x) = [\sin(x)]/x$, $(\Delta\omega_{dk}) = (\omega_{dk} - \hat{\omega}_{dk})$ is the Doppler shift tracking error (in radians) in the kth correlation interval, N is the number of samples in the correlation interval, $R(\cdot)$ is the autocorrelation function of the PRN code, ρ ($=|\tau - \hat{\tau}|/T_p$) is the normalised code phase tracking error, δ is the normalised code phase offset of the 'early' and 'late' code correlators of the DDLL, and D_{err} is the error component of D resulting from the reflected signal. From eqns. 1–4, D_{err} can be derived as

$$D_{err} = \frac{A^2}{4}\,\mathrm{sinc}^2[(\Delta\omega_{dk})N/2] \times \left\{\alpha^2\left[R^2\left(\rho-\delta+\frac{\Delta\tau_m}{T_p}\right) - R^2\left(\rho+\delta+\frac{\Delta\tau_m}{T_p}\right)\right] + 2\alpha\left[R(\rho-\delta)R\left(\rho-\delta+\frac{\Delta\tau_m}{T_p}\right) - R(\rho+\delta) \times R\left(\rho+\delta+\frac{\Delta\tau_m}{T_p}\right)\right]\cos[2\phi_c(k)+\beta]\right\} \quad (5)$$

where $\phi_c(k) \triangleq (\Delta\omega_{dk})N/2 + \phi(k-1)$ is the carrier phase residual at the centre of the kth correlation interval.

When $[(\Delta\omega_{dk})N/2]$ is time-invariant, the error component D_{err} depends on the multipath signal parameters α, $\Delta\tau_m$, β and the receiver design parameter δ of the DDLL. Because of the existence of D_{err}, the discriminator output $D \neq 0$ when $\rho = |\tau - \hat{\tau}| = 0$, which results in the DDLL locking at $|\tau - \hat{\tau}| = \tau_{err} \neq 0$, where τ_{err} is the root of the following equation

$$\frac{A^2}{4}\,\mathrm{sinc}^2[(\Delta\omega_{dk})N/2] \times \left[R^2\left(\frac{\tau_{err}}{T_p} - \delta\right) - R^2\left(\frac{\tau_{err}}{T_p} + \delta\right)\right] + D_{err} = 0 \quad (6)$$

τ_{err} can be obtained by solving eqns. 5 and 6. Fig. 2 shows τ_{err} as a function of $\Delta\tau_m$, α, ϕ_c and δ, respectively, from which we can conclude that: first, any reflected signal with additional code phase delay $\Delta\tau_m$ less than 1.5 code chips will cause the code phase tracking error τ_{err}. If $\Delta\tau_m$ is equal to or larger than 1.5 code chips, then the correlation between the direct-path signal and reflected signal disappears, which results in no tracking error due to the multipath. Secondly, with the increase of the amplitude coefficient α, the power of the reflected signal (relative to that of the direct-path signal) increases, therefore there is an increase in the code phase tracking error τ_{err}. Thirdly, τ_{err} is periodic with the carrier phase ϕ_c, and τ_{err} may be positive or negative depending on the carrier phase ϕ. Finally, the parameter δ of the code phase discriminator does not affect τ_{err} significantly.

Concerning the carrier phase tracking error due to the reflected signal $r_m(n)$, after the PRN code has been removed by the DDLL, the code-free in-phase and quadrature signals entering the DPLL in the kth correlation interval are

$$\bar{I}(k) = \frac{A}{2} R\left(\frac{\tau_{err}}{T_p}\right) \mathrm{sinc}\,[(\Delta\omega_{dk})N/2] \times \gamma \cos[\phi_c(k-1) + \psi]$$

$$\bar{Q}(k) = \frac{A}{2} R\left(\frac{\tau_{err}}{T_p}\right) \mathrm{sinc}\,[(\Delta\omega_{dk})N/2] \times \gamma \sin[\phi_c(k-1) + \psi] \quad (7)$$

where

$$\gamma = \left\{1 + \alpha^2\left[R\left(\frac{\tau_{err} + \Delta\tau_m}{T_p}\right)\Big/R\left(\frac{\tau_{err}}{T_p}\right)\right]^2 + 2\alpha\left[R\left(\frac{\tau_{err} + \Delta\tau_m}{T_p}\right)\Big/R\left(\frac{\tau_{err}}{T_p}\right)\right]\cos\beta\right\}^{0.5} \quad (8)$$

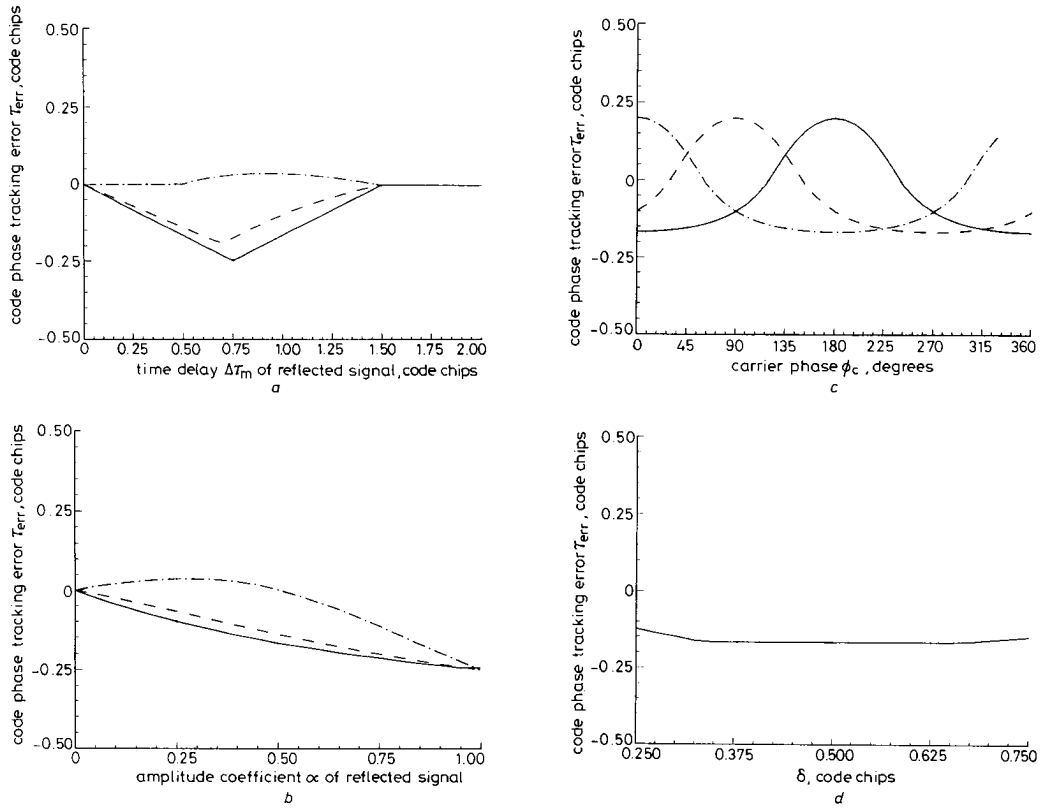

Fig. 2 *Code phase error plotted against multipath parameters*

a $\alpha = 0.5, \delta = 0.5, (\tau - \hat{\tau}) = 0.0, \beta = 0.2\pi$
——— $\phi_c = 0.0$ rad
— — $\phi_c = 1.0$ rad
—·—· $\phi_c = 2.0$ rad

b $\Delta\tau_m = 0.5, \delta = 0.5, (\tau - \hat{\tau}) = 0.0, \beta = 0.2\pi$
——— $\phi_c = 0.0$ rad
— — $\phi_c = 1.0$ rad
—·—· $\phi_c = 2.0$ rad

c $\Delta\tau_m = 0.5, \alpha = 0.5, \delta = 0.5, (\tau - \hat{\tau}) = 0.0$
——— $\beta = 0$
— — $\beta = \pi/2$
—·—· $\beta = \pi$

d $\Delta\tau_m = 0.5, \alpha = 0.5, (\tau - \hat{\tau}) = 0, \phi_c = 0.0, \beta = 0.2\pi$

is the amplitude change coefficient due to the reflected signal and

$$\psi = \tan^{-1}\left\{\frac{\alpha \dfrac{R((\tau_{err} + \Delta\tau_m)/T_p)}{R(\tau_{err}/T_p)} \sin\beta}{1 + \alpha \dfrac{R((\tau_{err} + \Delta\tau_m)/T_p)}{R(\tau_{err}/T_p)} \cos\beta}\right\} \quad (9)$$

is the input carrier phase shift due to the reflected signal, which can be proved to be the static carrier phase tracking bias. As shown in eqn. 9, with linear characteristics of the carrier phase discriminator, the amplitude change coefficient γ due to the reflected signal does not affect the output phase from the discriminator in the absence of noise. Fig. 3 shows the relationship between the carrier phase bias and the multipath parameters $\Delta\tau_m$, α and β, respectively, from which we observe that: first, the carrier phase tracking error ψ increases as the amplitude (αA) of the reflected signal $r_m(n)$ increases; secondly, the carrier phase tracking error ψ decreases as the code phase delay $\Delta\tau_m$ of $r_m(n)$ increases, because the correlation between the PRN codes of the direct-path and reflected signals decreases as $\Delta\tau_m$ increases, and the amplitude attenuation γ does not affect the DPLL phase tracking performance in the absence of input noise. Finally, the carrier phase tracking error ψ is periodic with phase shift β of reflected signal $r_m(n)$. The above theoretical analysis has been validated by computer simulations [8]. The analytic results can be extended to the case of multiple reflected signals, as discussed in the Appendix. If the actual multipath interference is a stochastic process described by its probability density function, it would be very difficult to solve eqn. 6 for τ_{err} and eqn. 9 for ψ. If the input noise is also considered, the theoretical analysis for τ_{err} and ψ would be impossible; therefore, in the following, we will study the multipath effects with the input noise based on computer simulation.

2.2 Multipath effects in the presence of noise

The above analytical results show the static errors of the GPS observables as functions of receiver design parameters and multipath signal parameters in the absence of input noise. We now discuss the dynamic errors (as functions of time) due to the multipath interference in the presence of input noise. For simplicity, only single reflection is considered. In the presence of noise, the nth sample of the DBP input signal is

$$i(n) = r_d(n) + r_m(n) + N(n) \quad (10)$$

where $N(\cdot)$ is the equivalent input Gaussian noise at baseband resulting from the receiver noise and antenna equivalent noise. Here only the direct-path signal component is taken as the signal component and the reflected signal is considered to be an interference component. Due to a low value of the carrier-to-noise density ratio (C/N_0) of the input GPS signals, the contribution of $r_m(n)$ to the power spectral density N_0 of noise at the receiver RF input is negligible compared with that of $N(n)$, therefore, the amplitude of $r_d(n)$ and the power spectral density N_0 of $N(n)$ are determined from the (C/N_0) value of the direct signal $r_d(n)$, and the parameters of the reflected signal $r_m(n)$ are determined from the parameters of $r_d(n)$ and the relative variation parameters α, $\Delta\tau_m$ and $\Delta\theta_m$. In the computer simulations, the input signal is controlled so that it is only contaminated by the equivalent input thermal noise $N(n)$ and the reflected signal $r_m(n)$, therefore, the multipath error can be analysed by comparison with the multipath-free situation (which is independent of errors from any other interference sources, such as ionosphere, troposphere, antenna phase centre movement,

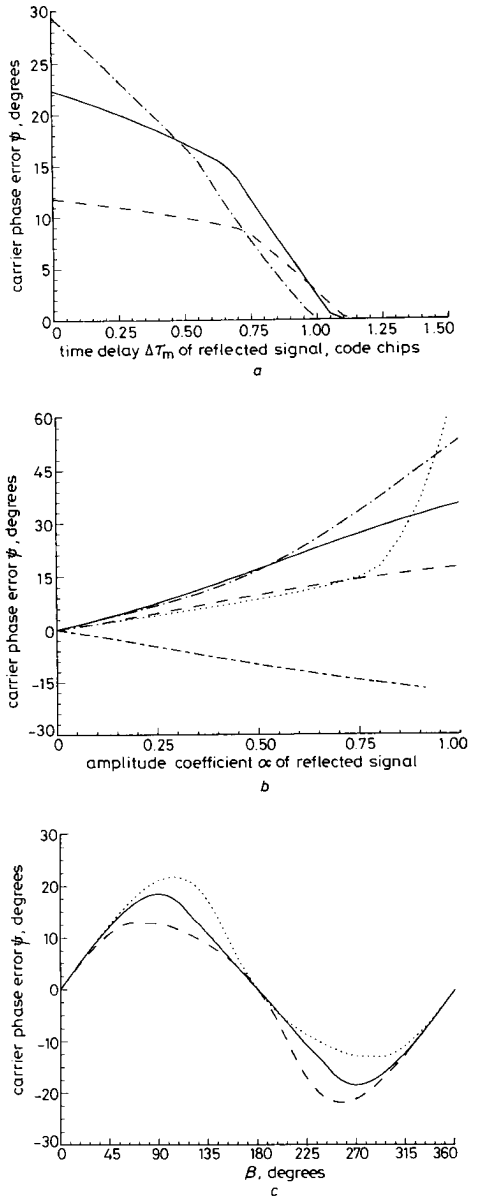

Fig. 3 *Carrier phase error plotted against multipath parameters*

a $\alpha = 0.5, \delta = 0.5, (\tau - \hat{\tau}) = 0.0, \Delta\theta_m = 0.0$
- — — $\beta = 0.2\pi$
- ——— $\beta = 0.4\pi$
- —·—· $\beta = 0.6\pi$

b $\Delta\tau_m = 0.5, \delta = 0.5, (\tau - \hat{\tau}) = 0.0, \Delta\theta_m = 0.0$
- — — $\beta = 0.2\pi$
- ——— $\beta = 0.4\pi$
- —·—· $\beta = 0.6\pi$
- ------- $\beta = 0.8\pi$
- —·—· $\beta = -0.2\pi$

c $\Delta\tau_m = 0.5, \alpha = 0.5, \delta = 0.5, (\tau - \hat{\tau}) = 0.0$
- ——— $\phi_c = 0.0$
- — — $\phi_c = 0.25\pi$
- ------- $\phi_c = -0.25\pi$

etc.). Fig. 4 shows the code phase tracking error $\tau_{err}(t)$ with a first-order DDLL (loop filter gain $G_1 = 0.4$ [7], $\delta = 0.5$) and a third-order DPLL (loop filter gains $G_1 = 0.8$, $r = 2.0$ and $P = 3.0$ [9]) for the first 10 s after $r_m(n)$ is

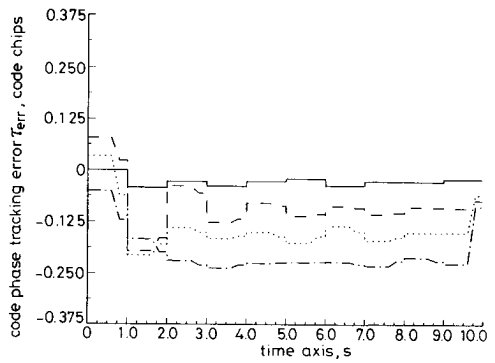

Fig. 4 *Code phase tracking error plotted against time (for a third-order DPLL)*

$G_1 = 0.8$, $r = 2.0$, $P = 3.0$, $\alpha = 0.5$, $\delta = 0.5$, $\beta = 0.2\pi$
——— $\Delta\tau_m = 0.1$
— — $\Delta\tau_m = 0.3$
····· $\Delta\tau_m = 0.5$
—·—· $\Delta\tau_m = 0.7$

added to the input signal $i(n)$. The correlation interval T is 20 ms, N is 43 036, and the code phase tracking (with carrier aiding [6]) from DDLL is updated by the DDLL every second. The code phase error is smooth with respect to time because the carrier aiding technique used in the code tracking loop can track the slow variations of the input code phase (compared with fast change rate of carrier phase), and also the code phase tracking error due to the input noise is dramatically reduced by the integrate-and-dump lowpass filter of very narrow bandwidth (1 Hz). The lowpass filter also causes the slight step change in $\tau_{err}(t)$ at the end of every second. Consequently, the code phase error (primarily resulting from the reflected signal $r_m(n)$) is steady with time as long as the multipath model is unchanged. Wherever a large steady error τ_{err} occurs (Fig. 4), there are obvious step changes at the end of each second because the transient responses of the code phase tracking process are longer than those with smaller steady error τ_{err}. $\tau_{err}(t)$ converges to the steady state value of τ_{err} which is validated by the analytic value obtained from eqns. 5 and 6. Fig. 5 shows the carrier phase tracking error $\psi(k)$ at the centre of the kth correlation interval averaged over a period of 0.2 s, with a first-order DDLL ($G_1 = 0.4$, $\delta = 0.5$), and a third-order DPLL ($G_1 = 0.8$, $r = 2.0$, $P = 3.0$). The multipath signal parameters are: $\alpha = 0.5$, $\Delta\tau_m = 0.1$ code chip width, and $\beta = 0.2\pi$ in case 1; $\alpha = 0.1$, $\Delta\tau_m = 0.5$ code chip width, and $\beta = 0.2\pi$ in case 2; $\alpha = 0.5$, $\Delta\tau_m = 0.5$ code chip width and $\beta = -0.2\pi$ in case 3. Unlike the noise-free case, the amplitude attenuation coefficient γ reduces the effective (C/N_0) of the input signal by γ^2 (which is 3 dB in this example). The phase tracking error consists of a random component due to input noise and a constant bias due to the reflected signal. In Fig. 5 the error components due to input noise is suppressed partly by the average operation on the phase error over every 0.2 s. Computer simulation results of observable errors due to the multipath with a first-order DDLL, second-order and third-order DPLLs are presented in [8] as functions of the multipath parameters, where the observable errors due to the multipath are averaged over a 10 s period to remove the effects of input noise. While the constant (or static) bias is common for both second-order and third-order DPLLs, the noise component is larger in the case of the third-order DPLL since a lower-order DPLL has better noise-suppression capability.

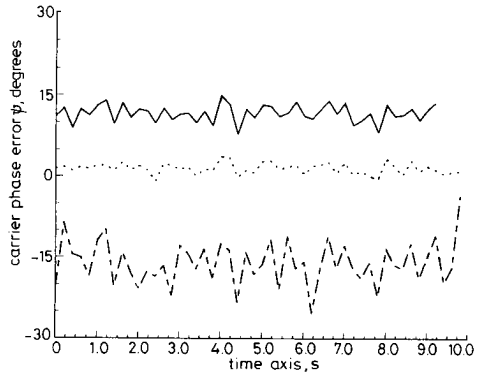

Fig. 5 *Carrier phase tracking error plotted against time with a third-order DPLL*

$G_1 = 0.8$, $r = 2.0$, $P = 3.0$, $\delta = 0.5$
——— case 1: $\alpha = 0.5$, $\Delta\tau_m = 0.1$, $\beta = 0.2\pi$
····· case 2: $\alpha = 0.1$, $\Delta\tau_m = 0.5$, $\beta = 0.2\pi$
- - - - case 3: $\alpha = 0.5$, $\Delta\tau_m = 0.5$, $\beta = 0.2\pi$

3 Effects of antenna characteristics

When a receiver is installed on board a ship, due to the dynamics of the ship the GPS observables are affected by the antenna residual phase (which varies with the azimuth and elevation angles of the satellites) and the antenna centre (to be defined) movement.

3.1 Effects of antenna residual phase

Practial GPS antennas cannot identically match the point-source characteristics in that the antenna phase response deviates from that of an ideal point source. The antenna performance may be described by the best-fit sphere (in the sense of least mean squares) and the resultant residual phase (which is the variation between the actual phase data and the best-fit sphere) [10]. The location of the centre of the best-fit sphere may be referred to as the antenna 'centre'. The residual phase is a function of the azimuth and elevation angles of the satellite signal as viewed from the receiving antenna. Many practical antennas have the difference between the maximum and minimum residuals larger than 60°, therefore, for high precision applications it is necessary to correct the carrier phase measurements based on the antenna residual phases. A simplified model of ship motions is chosen as the receiver dynamic pattern [11]. We consider the case that the ship undergoes rolling and pitching motion without translation. Assume that the elevation angle of the satellite to the antenna is

$$El(t) = El(0) - \theta_e \sin(\omega t) \tag{11}$$

where $El(0)$ is the elevation angle at $t = 0$, θ_e is the maximum elevation angle offset due to rolling and pitching, and ω is the composite radian frequency of the ship rolling and pitching. Assume also that the antenna 'centre' remains stationary. The dynamic parameters are taken as $El(0) = 57.40°$, $\theta_e = 30.00°$ and $\omega = 2\pi/8$ (rad). Fig. 6 is an example of measured GPS antenna residual

phases plotted against time which is obtained from a group of GPS antenna measurement data and from the ship dynamics. If we define $\theta_{ar}(t_k)$ as the antenna residual

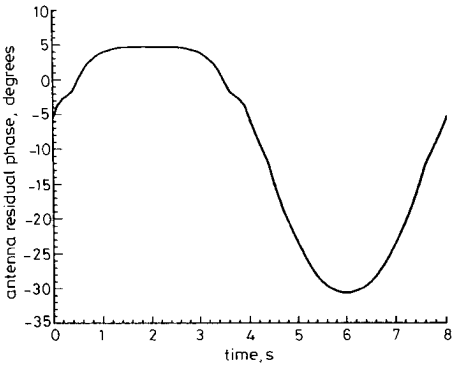

Fig. 6 *Antenna residual phase plotted against time*

phase at the end of the kth correlation interval t_k, then the differential antenna residual phase from t_{k-1} to t_k is

$$\Delta\theta_{ar} \triangleq \theta_{ar}(t_{k-1}) - \theta_{ar}(t_k) \tag{12}$$

Let $\theta_{lr}(t_k)$ and $\theta_{l0}(t_k)$ represent the carrier phases of the local numerically controlled oscillator (NCO) corresponding, respectively, to the situations when the antenna residual phase (Fig. 6) is taken into account and when no antenna residual phase is taken into account. Then the differential phase of $[\theta_{lr} - \theta_{l0}]$ at t_k is

$$\Delta\theta_l \triangleq [\theta_{lr}(t_{k-1}) - \theta_{l0}(t_{k-1})] - [\theta_{lr}(t_k) - \theta_{l0}(t_k)] \tag{13}$$

which presents the receiver dynanmic capability of tracking the variations of the antenna residual phase.

Figs. 7 and 8 show the comparison of the variations of the antenna residual phase and the local NCO carrier phase, with a first-order DDLL ($G_1 = 0.4$, $\delta = 0.5$), a second-order DPLL ($G_1 = 0.8$, $r = 2.0$ (Fig. 7)) and a third-order DPLL ($G_1 = 0.8$, $r = 2.0$ and $P = 3.0$ (Fig. 8)). The correlation intervals are chosen as: $T = 50$ ms, 200 ms and 500 ms. From these figures, we can conclude that: first, the effects of the input phase noise are very obvious when the input signal of the DPLLs has a low value of the signal-to-noise ratio (SNR), as when $T = 50$ ms. However, the noise effects decrease when the input SNR increases. Secondly, the local NCO tracks the residual phase with a time lag T, which is very obvious when $T = 500$ ms. Thirdly, compared with the second-order DPLL, the third-order DPLL has a shorter transient response duration and a larger transient tracking error. Finally, the receiver can track the variations of the antenna residual phase, i.e., the variations of the antenna residual phase will result in dynamic errors of the observable GPS phase. The low-frequency components of the antenna residual phase variations will appear at the observable phase and the error in the observable phase can be even larger than the antenna residual phase because of the transient phase tracking error. As a result, antenna residual phase corrections are necessary for high accuracy GPS positioning.

3.2 Effects of antenna centre movement

Fig. 9 shows the antenna centre movement due to the ship dynamics. Here we assume that the point 'O' (the intersection of the roll and pitch axes) is on the plane of the geocentre, the satellite and the antenna centre. The antenna centre moves along the arc 'abc' with the satellite elevation angle (viewed from the antenna) defined in eqn. 11. If the distance between the antenna centre and the point 'O' is H, then the distance between the antenna centre (at t) and the equiphase plane (of the antenna

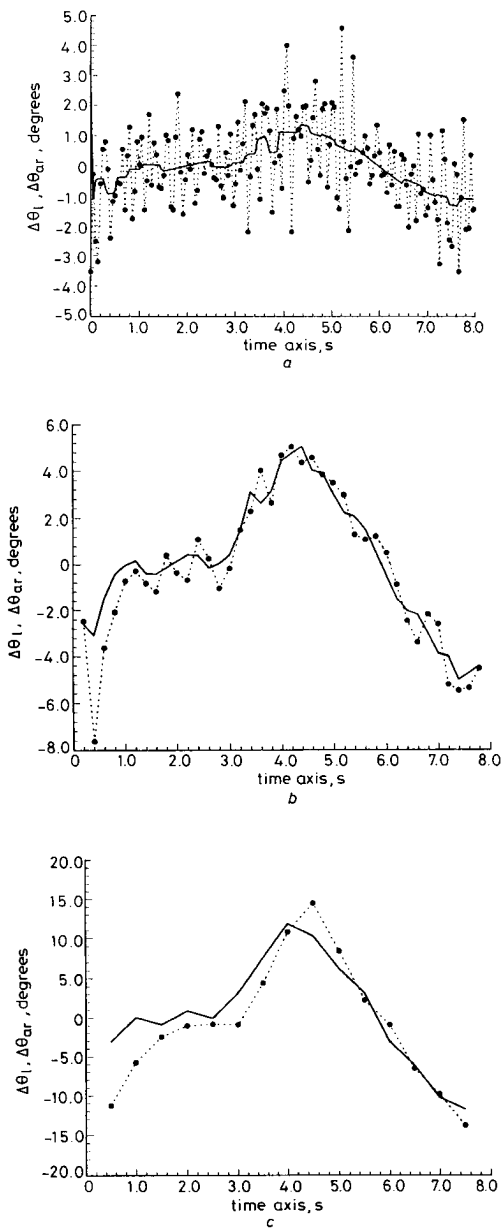

Fig. 7 *Comparison of variations of antenna residual phase and local NCO carrier phase with a first-order DDLL ($G_1 = 0.4$, $\delta = 0.5$) and a second-order DPLL*

····●···· $\Delta\theta_l$
——— $\Delta\theta_{ar}$
$G_1 = 0.8$, $r = 2.0$
a $T = 50$ ms
b $T = 200$ ms
c $T = 5000$ ms

centre at $t = 0$) is

$$d(t) = 2H \sin\left(\frac{\theta_e}{2} \sin \omega t\right) \cos\left[El(0) - \frac{\theta_e}{2} \sin \omega t\right] \quad (14)$$

and the variation of the Doppler frequency shift due to the ship dynamics is

$$\Delta f_d(t) = -\frac{f_L}{c} \omega H \theta_e \cos(\omega t) \cos El(t) \quad (15)$$

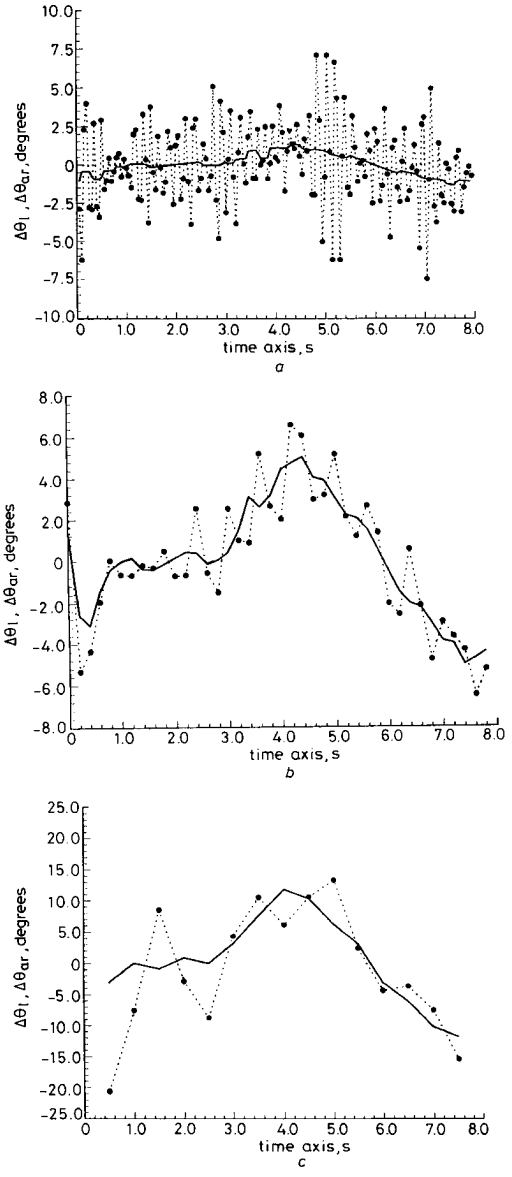

Fig. 8 *Comparison of variations of antenna residual phase and local NCO carrier phase with a first-order DDLL ($G_1 = 0.4$, $\delta = 0.5$) and a third-order DPLL*

···●··· $\Delta\theta_l$
——— $\Delta\theta_{ar}$
$G_1 = 0.8$, $r = 2.0$, $P = 3.0$
a $T = 50$ ms
b $T = 200$ ms
c $T = 500$ ms

where c is the velocity of electromagnetic waves in free space and $El(t)$ is defined in eqn. 11. The incoming signal

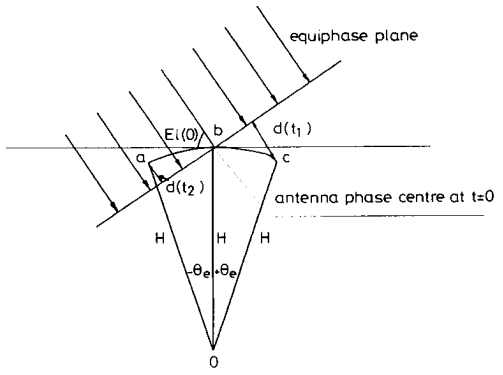

Fig. 9 *Antenna centre movement due to ship dynamics*

wavelength at the receiver antenna is

$$\lambda(t) = \frac{c}{f_L + f_d(t) + \Delta f_d(t)} \quad (16)$$

where $f_d(t)$ is the Doppler shift due to the satellite movement. The variations of the carrier phase and propagation time delay due to the ship dynamics are

$$\Delta\phi(t) \triangleq \phi(t) - \phi(0) = 2\pi\, d(t)/\lambda(t)$$
$$\Delta\tau(t) \triangleq \tau(t) - \tau(0) = d(t)/c \quad (17)$$

therefore, the ship dynamics result in the variations of the antenna residual phase, carrier phase, PRN code phases and Doppler shifts of the input signals (due to the antenna centre movement). Computer simulations are performed to analyse the effects of the ship dynamics on the GPS observables with a first-order DDLL ($G_1 = 0.4$, $\delta = 0.5$), a third-order DPLL ($G_1 = 0.8$, $r = 2.0$, $P = 3.0$) and the correlation interval $T = 50$ ms, where the dynamic parameters are $\omega = 2\pi/8$ rad, $H = 7.50$ m, $\theta_e = 30.00°$. The simulation results are given in Fig. 10, where $\Delta\theta_i$, $\Delta\tau_i$, and Δf_i are the variations of the carrier phase, pseudorange time delay and Doppler shift of the received signal due to the antenna centre movement, respectively; $\Delta\theta_l$, $\Delta\tau_l$ and Δf_l are the corresponding variations of the GPS observables obtained from the DDLL and DPLL. From the simulation results, we can observe that: first, the carrier phase tracking error due to input noise (on the order of degree) is negligible compared with that due to the antenna centre movement (on the order of cycle). The noise component is relatively so small that $\Delta\theta_l$ and $\Delta\theta_i$ overlap, as shown in Fig. 10*a*. Secondly, using the carrier-aiding technique, the DDLLs can track the variations of the code phase delays due to the receiver dynamics ($\Delta\tau_l$ and $\Delta\tau_i$ vary in a very similar pattern over each 1 s interval as shown in Fig. 10*b*), therefore, most of the phase tracking errors come from the input noise. Finally, Δf_l follows the variation of Δf_i to a great extent (Fig. 10*c*), i.e. the local NCO can track the variations of the input frequency. The errors due to the receiver dynamics are much larger than those due to the input noise. Other simulation parameters are also used. It is observed that, due to the receiver dynamics, the DPLL may lose lock if the bandwidth of the loop is not wide enough, for example, second- and third-order DPLLs cannot track the input carrier phase when $T = 0.5$ s (note that in this

case the antenna platform (ship) experiences only roll and pitch with no translation). In general, since the variations may contain large DC components because of the dynamic environments, the variations of the code phase delay, carrier phase and frequency cannot be removed in postprocessing of the GPS observables simply by lowpass filters, as is usually done to remove the error components due to white noise. Further processing may be necessary to remove the errors of the observables (due to antenna dynamics) for accurate positioning.

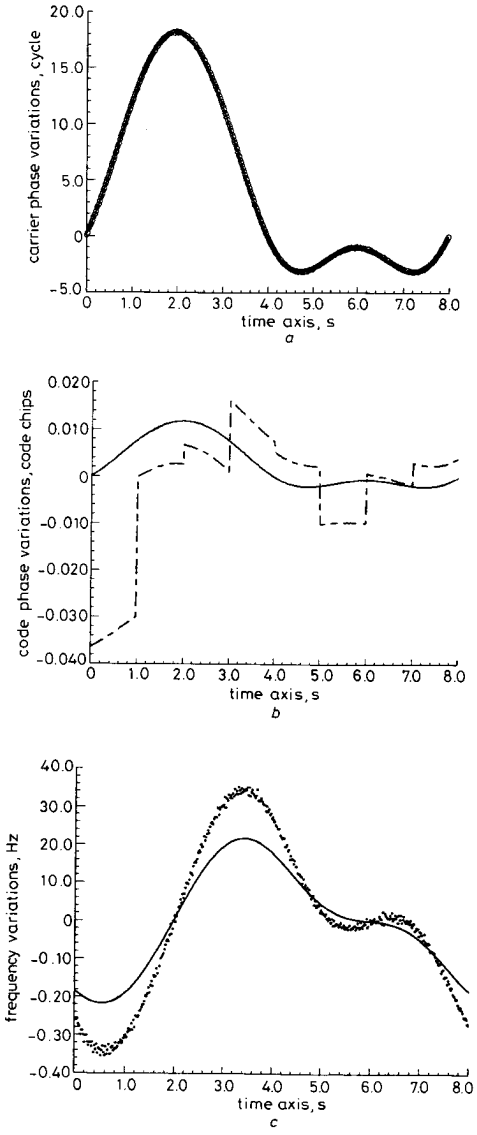

Fig. 10 *Comparison of variations of GPS observables and input signal parameters (T = 50 ms) with a first-order DDLL (G_1 = 0.4, δ = 0.5) and a third-order DPLL (G_1 = 0.8, r = 2.0, P = 3.0)*

a carrier phase variations
○ $\Delta\theta_i$
—— $\Delta\theta_i$
b code phase variations
— — $\Delta\tau_i$
—— $\Delta\tau_i$
c frequency variations
—— Δf_i
• Δf_i

4 Conclusions

In this paper, we have applied the functional modelling and software package of the digital baseband processor to illustrate the dependence of the observable accuracy of the GPS receiver on the multipath signal parameters, the GPS antenna characteristics, the receiver structures and design parameters. The software package can be used as an effective tool in designing and developing a GPS receiver, and in analysing the effects of the system dynamics (including those of both satellite and user receiver), and the signal propagation media (such as ionosphere, troposphere, multipath, and GPS receiver antenna) on the GPS observables. Computer simulation using the software receiver is more accurate in the sense that the effects of each interference source, receiver parameter and system dynamic parameter can be isolated and analysed separately, and that the characteristics of the input interference are known exactly. These conditions are impossible to specify with hardware receivers. The software receiver provides an additional approach to the research on the positioning accuracy of the GPS.

5 References

1 GETTING, I.A.: 'The global position system', *IEEE Spectrum*, 1993, **30**, (12), pp. 36–47
2 SCHUCHMAN, L., ELROD, B.D., and VAN DIERENDONCK, A.J.: 'Applicability of an augmented GPS for navigation in the National Airspace system', *Proc. IEEE*, 1989, **77**, (11), pp. 1709–1727
3 GEORGIADOU, Y., and KLEUSBERG, A.: 'Ionospheric refraction and multipath effects in GPS carrier phase observations'. Proceedings of IUGG XIX General Assembly, Symposium U3, Vancouver, B.C., Canada, 1987
4 BLETZACKER, F.R.: 'Reduction of multipath contamination in a geodetic GPS receiver'. Proceedings of the First International Symposium on Precise Positioning with the Global Positioning System, Rockville, MD, USA, 1985. Vol. I, pp. 413–422
5 EVANS, A.G.: 'Comparison of GPS pseudorange and biased Doppler range measurements to demonstrate signal multipath effects'. Proceedings of the Fourth International Symposium on Satellite Positioning, Austin, TX, USA, 1986, pp. 573–578
6 ZHUANG, W., and TRANQUILLA, J.: 'Digital baseband processor for the GPS receiver — modelling and simulations', *IEEE Trans.*, 1993, **AES-29**, (4), pp. 1343–1349
7 ZHUANG, W., and TRANQUILLA, J.: 'Modeling and analysis for the GPS pseudorange observable', *IEEE Trans. on Aerosp. Electron. Syst.*, 1995, **31**, (2), pp. 739–751
8 ZHUANG, W., and TRANQUILLA, J.: 'Multipath effects on the GPS observables'. Proceedings of the Sixteenth Biennial Symposium on Communications, Kingston, Ontario, Canada, 1992, pp. 454–457
9 ZHUANG, W.: 'Composite GPS receiver modelling, simulations and applications'. PhD dissertation, Department of Electrical Engineering, University of New Brunswick, Fredericton, NB, Canada, October 1992
10 TRANQUILLA, J.M., and COLPITTS, B.G.: 'GPS antenna design characteristics for high precision applications'. Proceedings of the Engineering Applications of GPS Satellite Surveying Technology, Nashville, TN, 1988
11 BLAGOVESHCHENSKY, S.N.: '*Theory of ship motions*' (Dover, New York, 1962)

6 Appendix

Define α_i as the amplitude ratio of the ith reflected signal to direct-path signal, $\Delta\tau_{mi}$ as the additional time delay of the ith reflected signal with respect to the direct-path signal, and $\Delta\theta_m$ as the carrier phase shift induced by the ith reflector, and let $\beta_i = -(\omega_b + \omega_d)\,\Delta\tau_m/T_s + \Delta\theta_{mi}$, then

the received multipath signal is

$$r_m(n) = \sum_{i=1}^{M} \alpha_i AP[(1+\zeta)nT_s - \xi T_p + \Delta\tau_{mi}] \times \cos[(\omega_b + \omega_{dk})n + \phi(k-1) + \beta_i] \quad (18)$$

where M is the total number of multiple paths taken into account. The multipath signal generates the following error in the output of the PRN code phase discriminator

$$\begin{aligned} D_{err} = \frac{A^2}{4} \operatorname{sinc}^2[(\Delta\omega_{dk})N/2] \\ \times \left\{ \sum_{i=1}^{M} [\alpha_i R(\rho - \delta + \Delta\tau_{mi}/T_p)]^2 \right. \\ - \sum_{i=1}^{M} [\alpha_i R(\rho + \delta + \Delta\tau_{mi}/T_p)]^2 \\ + \sum_{\substack{i,j=1 \\ i \neq j}}^{M} \alpha_i \alpha_j \cos(\beta_i - \beta_j)[R(\rho - \delta + \Delta\tau_{mi}/T_p) \\ \times R(\rho - \delta + \Delta\tau_{mj}/T_p) - R(\rho + \delta + \Delta\tau_{mj}/T_p) \\ \times R(\rho + \delta + \Delta\tau_{mj}/T_p)] + 2R(\rho - \delta) \\ \times \sum_{i=1}^{M} \alpha_i R(\rho - \delta + \Delta\tau_{mi}/T_p) \cos[2\phi_c(k) + \beta_i] \\ - 2R(\rho + \delta) \sum_{i=1}^{M} \alpha_i R(\rho + \delta + \Delta\tau_{mi}/T_p) \\ \left. \times \cos[2\phi_c(k) + \beta_i] \right\} \end{aligned} \quad (19)$$

The PRN code phase tracking error due to the multipath reflections can be computed by substituting D_{err} of eqn. 19 into eqn. 6 and solving for τ_{err}. For carrier phase tracking, the amplitude change coefficient due to the multiple reflections is

$$\gamma = \left\{ \left[1 + \sum_{i=1}^{M} \alpha_i \frac{R\left(\frac{\tau_{err} + \Delta\tau_{mi}}{T_p}\right)}{R\left(\frac{\tau_{err}}{T_p}\right)} \cos\beta_i \right]^2 + \left[\sum_{i=1}^{M} \alpha_i \frac{R\left(\frac{\tau_{err} + \Delta\tau_{mi}}{T_p}\right)}{R\left(\frac{\tau_{err}}{T_p}\right)} \sin\beta_i \right]^2 \right\}^{0.5} \quad (20)$$

which does not affect the output of the carrier phase discriminator in the noise-free case. The input carrier phase shift due to the multiple reflections is, in modulo 2π sense

$$\psi = \arctan \left\{ \left[\sum_{i=1}^{M} \alpha_i \frac{R\left(\frac{\tau_{err} + \Delta\tau_{mi}}{T_p}\right)}{R\left(\frac{\tau_{err}}{T_p}\right)} \sin\beta_i \right] \div \left[1 + \sum_{i=1}^{M} \alpha_i \frac{R\left(\frac{\tau_{err} + \Delta\tau_{mi}}{T_p}\right)}{R\left(\frac{\tau_{err}}{T_p}\right)} \cos\beta_i \right] \right\} \quad (21)$$